

Research Article

Design and Analysis of the Waste Heat Recovery System for Stenter Exhaust

Yimin Chen, Bo Liu, Zheng Zeng*, Liqing Li*, 

School of Energy Science and Engineering, Central South University, Changsha 410083, Hunan, China
E-mail: zengzheng@csu.edu.cn (Z.Z.); liqingli@hotmail.com (L.L.)

Received: 27 October 2023; **Revised:** 21 February 2024; **Accepted:** 27 February 2024

Abstract: In this study, combined with the exhaust adsorption, desorption and catalytic combustion technology, a waste heat recovery scheme using stenter exhaust to heat desorbed air and preheat stenter suction air was proposed. Using Aspen Plus to design the waste heat recovery system, and using Aspen EDR to design the structure of heat exchangers. The energy utilization efficiency of waste heat recovery system was evaluated through the exergy analysis, and the influence of exhaust flow rate variation on exergy efficiency of heat exchanger under different exhaust temperatures were discussed. Moreover, the influence of fluid parameter variations on the heat transfer process was also analyzed. Finally, the economic calculation was carried out and the overall energy-saving effect of waste heat recovery system was demonstrated. The results showed that the utilization of this waste heat recovery system can recover 537 kW, the exergy efficiency of desorbed air heat exchanger and preheating air heat exchanger were 51% and 58.9% respectively. In terms of the economic evaluation, the annual energy-saving economic benefits was about \$ 89,312, and the static investment payback period was 1.17 years.

Keywords: Stenter exhaust; Low grade waste heat recovery; Heat exchanger design; Thermal analysis

1. Introduction

China is a major player in textile industry, producing a large amount of textiles every year while also causing increasingly serious environmental problems due to the emissions of waste gas [1]. During the textile production process, a large amount of dyes and solvents are used. After mixing with other organic compounds such as grease and wax in other process steps, these solvents volatilize under high temperatures in thermofixation section, forming complex waste gas with various volatile organic compounds (VOCs). Among them, xylene, formaldehyde and toluene, as the main sources of ozone formation, have an obvious impact on the air quality [2]. Therefore, it is necessary to remove VOCs in exhaust gas.

In terms of various methods for treating VOCs, including biolysis, photocatalysis, membrane separation, and plasma catalysis, each with their own limitations [3–5]. Compared to a single treatment method, a combination of VOCs treatment technologies is more effective for VOCs treatment. For the characteristics of high air volume and low VOCs concentration in stenter exhaust, exhaust adsorption, desorption and catalytic combustion technology can be adopted for economic and environment-friendly treatment [6]. In the desorption stage, the desorbed gas needs to be heated up to achieve an appropriate temperature, herein, the heating energy can be provided by the waste heat recovery of stenter exhaust.

The stenter typically operates at temperatures ranging from 120–210 °C, with exhaust temperatures between 100–190 °C [7]. Despite being a low-grade heat source compared to the ambient temperature of 30 °C, the total amount of waste heat produced is large. Direct discharging the exhaust into the atmosphere would result in massive energy losses. Given the low energy utilization efficiency of stenter, it is crucial to study the potential for

waste heat recovery from its exhaust and design a recovery plan. By adopting waste heat recovery technology, factories can improve energy utilization efficiency and reduce environmental pollution [8]. For the waste heat recovery of stenter exhaust, various types of heat exchangers and heat recovery methods have been developed [9]. Some researches show that using waste heat of stenter exhaust to preheat air can save 10% and 13.6% energy consumption [10–11]. The production practice shows that using waste gas heat recovery system leads to a huge difference in energy consumption [12].

The exhaust emissions from stenter contain various VOCs, which has a great impact on the air quality and human health. However, the exhaust with temperatures ranging from 100 to 190 °C has rarely been reported in term of the heat recovery potential. Based on the dual characteristics of the exhaust, it can be effectively treated using exhaust adsorption, desorption, and catalytic combustion technology, along with waste heat recovery technology. The waste heat recovery process is established using Aspen Plus, and an exergy analysis of the process is conducted through analyzing the parameters of each stream. Simultaneously, the impact of variations in the exhaust under different operating conditions on the waste heat recovery process is explored. Finally, detailed structures for the heat exchangers are designed, economic benefits of the waste heat recovery project are analyzed, and the overall energy-saving effect of exhaust waste heat recovery system is demonstrated.

2. Model of Waste Heat Recovery Process of Stenter Exhaust

2.1 Exhaust Treatment Process Description

Using exhaust adsorption, desorption and catalytic combustion technology can effectively remove most of the VOCs in waste gas and use the concentrated VOCs for catalytic combustion to improve economic benefits. The exhaust treatment process is shown in Figure 1. In the adsorption process, the exhaust undergoes pretreatment to remove particles such as oil droplets and dust, and then enters double fixed-beds adsorber for VOCs adsorption. In the desorption process, the saturated adsorber is desorbed and regenerated, and the desorbed high-concentration VOCs are transported to the fixed-bed catalytic reactor for the catalytic combustion.

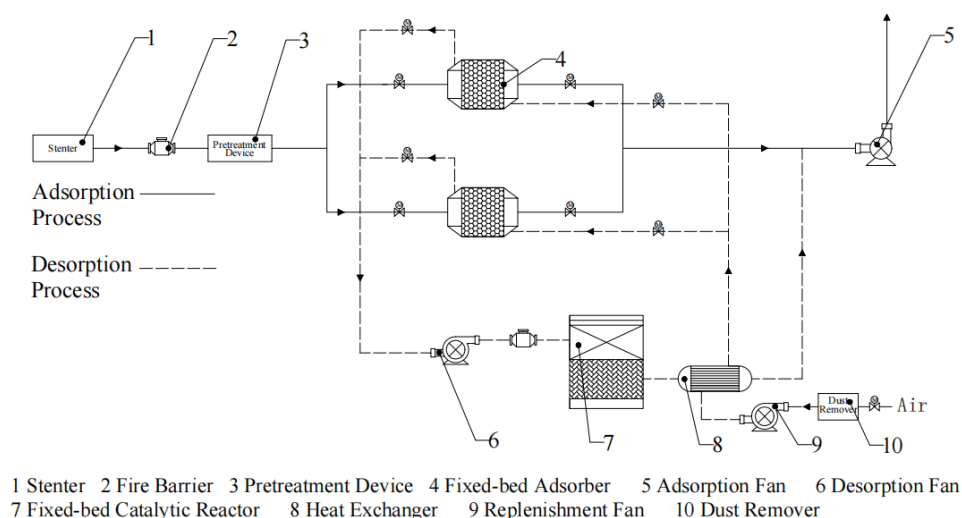


Figure 1. The schematic of the treatment process of stenter exhaust.

In general, the temperature of adsorbed gas should not exceed 40 °C. If the gas temperature is too high, the adsorption performance of the adsorbent will decrease prominently. Therefore, a heat recovery process can be added before the adsorption process to reduce the exhaust temperature. Due to the limitations of stenter exhaust treatment process, the exhaust temperature is reduced to 90 °C after the heat recovery, to avoid clogging pipes by oil mist condensation caused by excessive cooling. Then, the exhaust gas is subjected to a pretreatment process to remove impurities and to lower the temperature to below 40 °C before entering the fixed-beds adsorber.

In the traditional catalytic combustion process, the desorbed air will be heated by the energy generated by the catalytic combustion of concentrated VOCs. After adding the heat recovery process, part of the heat obtained will be used to heat the desorbed air instead, and the other part will be used to preheat the stenter suction air.

2.2 Waste Heat Recovery Process Establishment

The composition of the stenter exhaust is complex, including more than 30 kinds of VOCs such as xylene, benzene, and toluene. Considering that VOCs account for only a small part of the waste gas composition, usually with a concentration range of 0~20 mg/m³, the influence of VOCs on the heat transfer process can be ignored, and the waste gas can be regarded as air. The PENG-ROB calculation method is chosen, which is suitable for non-polar or weakly polar mixed systems at all temperatures and pressures [13].

The temperature was measured by 1.5 mm thermo-elements of Ktype. The pressure and flow rate were measured by a Kistler ThermoComp quartz sensor. And various kinds of VOCs were measured by Model SP-2000 gas chromatograph. The exhaust flow rate is measured as 30,000 m³/h, as treated as ideal gas, converting to a molar flow rate of 825.4 kmol/h. In the desorption process, the desorbed air flow is usually one quarter of the adsorbed gas. The stenter suction air is preheated by waste heat recovery and further heated by the heater to reach the original stenter exhaust temperature, and then enters the stenter for a new working cycle. Therefore, the stenter suction air flow rate is set to be equal to the exhaust flow rate, and both desorbed air and stenter suction air come from the environment. The initial stream parameters of the heat transfer process are listed in Table 1.

Table 1. Initial parameters of each stream.

| Stream Category | Temperature (°C) | Pressure (atm) | Flow Rate (kmol/h) |
|---------------------|------------------|----------------|--------------------|
| Stenter exhaust | 170 | 1 | 825.4 |
| Desorbed air | 30 | 1 | 206.4 |
| Stenter suction air | 30 | 1 | 825.4 |

The waste heat recovery system is composed of desorbed air heat exchanger (E1), preheating air heat exchanger (E2), heater (H1). For E1, its goal is to produce hot air for VOCs desorption. Due to the desorption temperature of the adsorbent typically being between 100~110 °C, the outlet temperature of the cold stream is set to be 100 °C. For E2, its goal is to fully recover the remaining waste heat to preheat stenter suction air after first heat exchange. After the heat recovery, the exhaust gas temperature drops to 90 °C, therefore the temperature difference between the outlet of hot stream and the inlet of cold stream is set to be 60 °C. For H1, its goal is to further heat up the stenter suction air to reach the original stenter exhaust temperature.

The overall simulation calculation parameters are listed in Table 2.

Table 2. Overall simulation calculation parameters.

| Component | Calculation Method | | |
|--------------------|--------------------------------|--|----------|
| | Base Method | Air Peng-ROB | |
| Exchangers Model | | | |
| Name | E1 | E2 | H1 |
| module | HeatX | HeatX | Heater |
| Type | GEN-HT | GEN-HT | HEATER |
| Fidelity | short cut | short cut | - |
| Calculation mode | design | design | - |
| Flow direction | countercurrent | countercurrent | - |
| Specification | Cold stream outlet temperature | Hot outlet-cold inlet temperature difference | - |
| Value | 100 °C | 60 °C | - |
| Outlet Temperature | - | - | 170 °C |
| Outlet Pressure | - | - | 1 atm |
| Utility | - | - | HP Steam |

In term of the assumptions of this model, the water vapor was excluded. Consequently, the enthalpy change of the water vapor condensation is not considered. This assumption is reasonable only when the moisture content in the exhaust is relatively low. While the waste heat recovery model explores the impact of exhaust conditions, such as temperature and flow rate, on the recovery process, it does not account for changes in exhaust pressure during this process, which may have influences for the waste heat recovery process.

3. Simulation Analysis of Waste Heat Recovery Process

3.1 Simulation Result

Through the establishment of the above model, the simulation results obtained by calculation are shown in Figure 2.

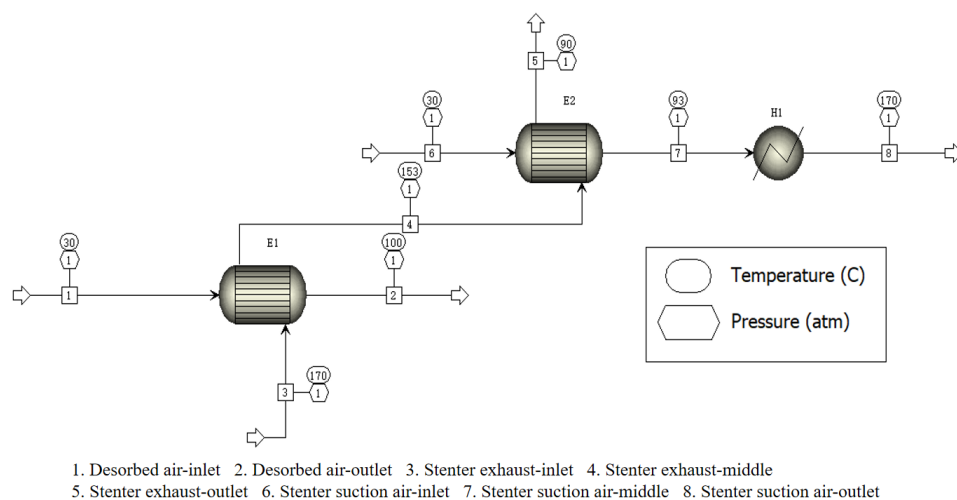


Figure 2. The flow chart of simulation results of waste heat recovery system.

According to Figure 2, the exhaust and desorbed air enter the desorbed air heat exchanger (E1). Desorbed air is discharged from E1 after being heated to 100 °C, while the exhaust temperature drops to 153 °C. Then the exhaust enters the preheating air heat exchanger (E2) for heat exchange with the stenter suction air, making full use of the remaining waste heat in the exhaust. Finally, the exhaust temperature drops to 90 °C before being discharged. The stenter suction air is heated to 93 °C after the heat exchange, then further heated to 170 °C through the heater (H1), and finally enters the stenter. The calculation results show that the thermal load of E1 is 117 kW, the thermal load of E2 is 420 kW, and the thermal load of H1 is 517 kW.

3.2 Exergy Analysis of Waste Heat Recovery Process

The thermodynamic parameters of each stream in the process can be obtained from Results Summary, to facilitate subsequent calculation, all the parameters are summarized in Table 3.

Table 3. Thermodynamic parameters of each stream.

| Stream Category | Flow Rate (kmol/h) | Temperature (°C) | Pressure (atm) | Molar Enthalpy (kJ/kmol) | Molar Entropy (kJ/kmol·K) |
|-----------------|--------------------|------------------|----------------|--------------------------|---------------------------|
| EX--IN | 825.4 | 170 | 1 | 4222.2 | 11.54 |
| EX-M | 825.4 | 153 | 1 | 3713.06 | 10.36 |
| EX-OUT | 825.4 | 90 | 1 | 1881.94 | 5.71 |
| AIR1-IN | 206.4 | 30 | 1 | 136.88 | 0.46 |
| AIR1-OUT | 206.4 | 100 | 1 | 2173.41 | 6.50 |
| AIR2-IN | 825.4 | 30 | 1 | 136.88 | 0.46 |
| AIR2-M | 825.4 | 93 | 1 | 1968.00 | 5.95 |
| AIR2-OUT | 825.4 | 170 | 1 | 4222.2 | 11.54 |

Note: AIR1 represents desorbed air, AIR2 represents stenter suction air.

Common energy analysis methods include the thermal performance analysis combining heat transfer and pressure drop, entropy analysis, exergy analysis, etc [14–16]. Among them, the exergy analysis reveals energy flow processes from the perspective of energy quality, which can comprehensively identify the reasons for the decrease in energy quality during the energy transfer, to evaluate the energy utilization efficiency of the system. Based on the data in Table 3, the exergy analysis method is used to analyze the waste heat recovery process, with the following calculations.

The waste heat recovery process does not involve chemical reactions, so the chemical exergy of the fluid is ignored, and the physical exergy of the fluid is focused. The expression for the exergy loss caused by the heat transfer temperature difference between the hot and cold fluids can be represented as [17]:

$$E_T = E_h + E_c \quad (1)$$

$$E_h = T_0(S_{h,out} - S_{h,in}) \quad (2)$$

$$E_c = T_0(S_{c,out} - S_{c,in}) \quad (3)$$

ET (kJ) represents exergy loss of the system, Eh and Ec respectively represent exergy change of hot and cold fluid after heat transfer, Sout and Sin (kJ/K) represent entropy of outlet and inlet respectively, and T0 (K) represents the ambient temperature.

Exergy efficiency of the heat exchanger η_{ex} (%) is represented as:

$$\eta_{ex} = \frac{Ex_{c,out} - Ex_{c,in}}{Ex_{h,in} - Ex_{h,out}} \quad (4)$$

Exc,out and Exc,in represent exergy value at the exit and entry of cold fluid respectively, while Exh,in and Exh,out represent exergy value at the entry and exit of hot fluid respectively.

EUR is defined as the Exhaust Exergy Utilization Rate [18], indicating the proportion of exergy recovered by the cold fluid to the total exergy of the hot fluid. It is employed to characterize the utilization of exergy from the exhaust in waste heat recovery systems.

$$EUR = \frac{Ex_{c,out} - Ex_{c,in}}{Ex_{h,in}} \quad (5)$$

0 °C and 1 atm are used as the ground state to calculate the exergy value of each stream. The relative exergy value of each stream is obtained by calculating the data in Table 3, and the exergy flow diagram of waste heat recovery process is drawn, as shown in Figure 3.

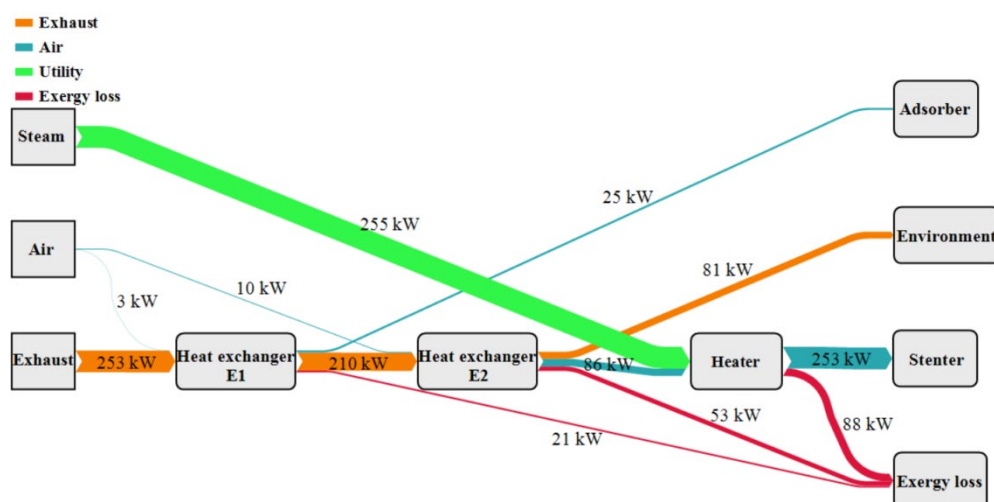


Figure 3. Exergy flow diagram of waste heat recovery process.

According to Figure 3, the exergy value of exhaust decreases from 253 kW to 81 kW after two rounds of heat exchange, a reduction of 172 kW. The exergy value of stenter suction air increases from 10 kW to 86 kW after the heat exchange, an increase of 76 kW. The total exergy loss in waste heat recovery process is 162 kW.

Table 4. Exergy analysis of waste heat recovery system.

| | E1 | E2 | H1 | System |
|-----------------------|-----|------|------|--------|
| Exergy loss (kW) | 21 | 53 | 88 | 162 |
| Exergy efficiency (%) | 51 | 58.9 | 65.5 | 68.9 |
| EUR(%) | 8.7 | 30 | - | - |

The exergy analysis of waste heat recovery process is summarized in Table 4. It can be seen that the exergy efficiency of E1 is relatively low. This is mainly because the large temperature difference between the hot and cold fluids in heat exchange process, resulting in a high local heat transfer rate. At the outlet of the heat exchanger,

the temperature difference between the hot and cold fluids reaches a minimum value of 70 °C, which is still higher than the fixed heat transfer temperature difference of 60 °C in E2, resulting in a greater exergy loss. The utility of H1 uses medium-pressure steam with a temperature of 250 °C and a pressure of 39 atm, achieving a good exergy efficiency. The EUR for E1 and E2 are 8.7% and 30%, respectively. This indicates that the heat recovered from the desorbed air constitutes a relatively small proportion of the total exergy of the waste heat, primarily due to the limitations imposed by the low flow rate of the desorbed air. The combined exergy recovery from both processes accounts for 38.7% of the total waste heat exergy.

3.3 Analysis of Factors in Heat Transfer Process

The function of the waste heat recovery system is not only to obtain high temperature desorption air, but more importantly, to recover the waste heat of the exhaust as much as possible. Due to the limitation of the stenter exhaust treatment process, the exhaust temperature finally drops to a minimum of 90 °C, and then exhaust enters the next treatment stage. The exhaust exergy from 90 °C to the ambient temperature cannot be utilized. Therefore, it is more practical to discuss how to improve the exergy efficiency of heat exchanger E1, retain more exhaust available energy after the first heat exchange.

The reason for the low heat utilization efficiency of E1, in addition to the large temperature difference between the cold and hot fluids, is also influenced by the flow rate difference between the cold and hot fluid in the heat transfer process. Since the flow rate of the cold fluid is one-fourth that of the hot fluid, the cold fluid will heat up rapidly while the hot fluid cools down slowly during the heat transfer process. Therefore, the hot fluid only decreases by 17 °C after heat transfer process. Reducing the flow rate of the hot fluid can significantly reduce its temperature and lower the mean temperature difference in the heat transfer process, thereby increasing the exergy efficiency of E1. The relationship diagram is shown as Figure 4.

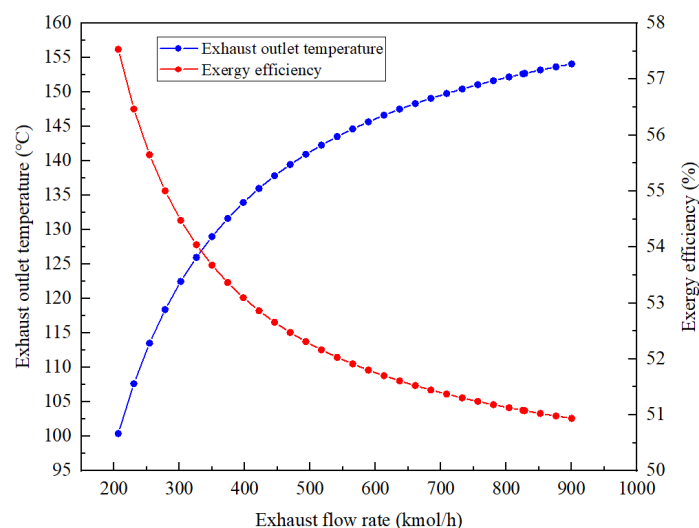


Figure 4. Variations of exhaust outlet temperature and exergy efficiency of heat exchanger E1 with exhaust flow.

As shown in Figure 4, when exhaust flow rate is much higher than desorbed air one, exhaust outlet temperature slowly decreases as exhaust flow rate decreases. At this point, the exergy efficiency of E1 is low, mainly because the average heat transfer temperature difference during heat transfer process is large, and the heat transfer rate is high, resulting in significant irreversible losses [19]. When exhaust flow rate decreases to a level close to desorbed air one, the exhaust outlet temperature decreases significantly. In reverse, the exergy efficiency increases significantly.

Note that, when the exhaust flow rate is 278 kmol/h, the heat recovery efficiency of E1 can reach 55%, representing a 4% improvement compared to the original heat exchanger efficiency. Therefore, employing a bypass strategy by dividing the exhaust stream into three equal flows for separate heat recovery could theoretically enhance the overall energy utilization efficiency of the waste heat recovery system.

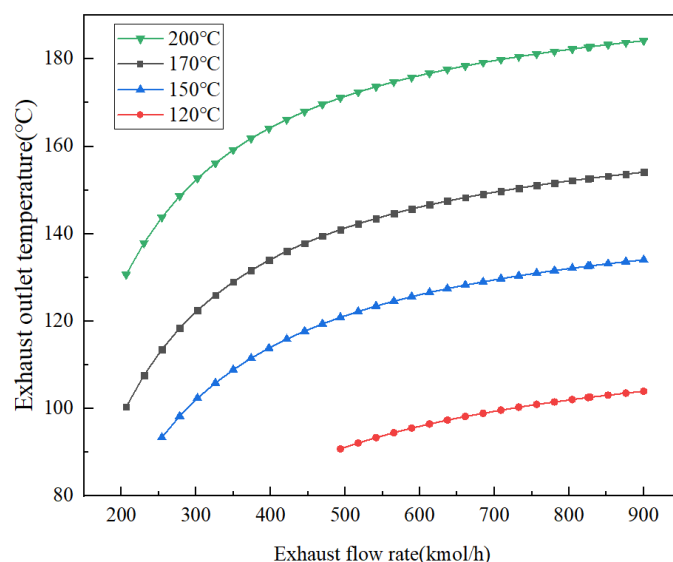


Figure 5. The variations in exhaust outlet temperature with changes in exhaust flow rate at different exhaust temperatures.

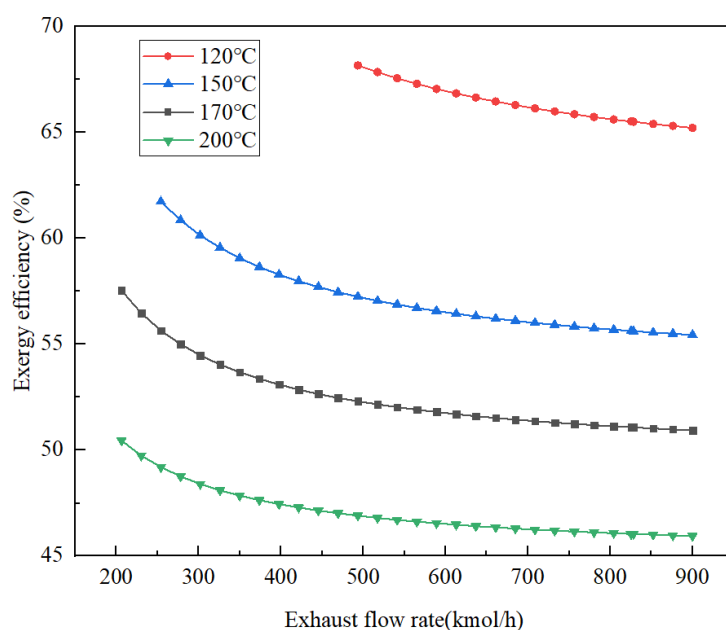


Figure 6. The variations in E1 exergy efficiency with changes in exhaust flow rate at different exhaust temperatures.

Table 5. The differences in E1 exergy efficiency after adopting the bypass strategy at different exhaust temperatures.

| Exergy efficiency (%) | | | |
|-----------------------|--------|--------|--------|
| | 150 °C | 170 °C | 200 °C |
| 825 kmol/h | 825 | 51.0 | 46.0 |
| 278 kmol/h | 278 | 55.0 | 48.7 |

Going further, Figures 5 and 6 are used to explore the variations in exhaust outlet temperature and E1 exergy efficiency with changes in exhaust flow rate at different exhaust temperatures. Notably, at an exhaust temperature of 120 °C, when the exhaust flow rate decreases to 493 kmol/h, the exhaust outlet temperature drops to 90 °C. However, due to constraints in the exhaust treatment technology, the temperature cannot be further reduced. Throughout the process of reducing the exhaust flow rate from 825 kmol/h to 493 kmol/h, the E1 exergy efficiency increases from 65.5% to 68.1%. Comparing the differences in E1 exergy efficiency after adopting the bypass

strategy at exhaust temperatures of 150 °C, 170 °C, and 200 °C, the results are presented in Table 5. At an exhaust temperature of 150 °C, the E1 exergy efficiency reaches the greatest improvement after adopting the bypass strategy. However, the exhaust outlet temperature decreases to 98 °C meanwhile, which represents a relatively small temperature difference that may be unfavorable for subsequent heat exchange. At an exhaust temperature of 170 °C, adopting the bypass strategy results in a noticeable improvement in E1 exergy efficiency, with the exhaust outlet temperature decreasing to 118 °C. This choice still maintains a reasonable heat exchange temperature difference. Therefore, if the bypass strategy is used, selecting an exhaust temperature of 170 °C will be more appropriate.

Comparing the E1 exergy efficiency at an exhaust flow rate of 825 kmol/h across different temperature levels, it is evident that there is a significant difference in exergy efficiency among various temperature grades. With each reduction in temperature level, there is an approximate 5% improvement in exergy efficiency. This suggests that theoretically pursuing a 4% increase in exergy efficiency through the adoption of the bypass strategy is a substantial benefit.

The variation of exhaust flow rate will also change the outlet temperature of stenter suction air. In order to guide the adjustment of exhaust flow rate, The relationship diagram is drawn as shown in Figure 7.

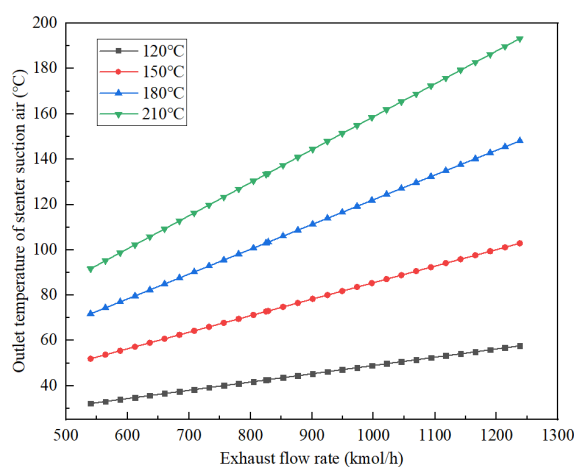


Figure 7. Variation of outlet temperature of stenter suction air with exhaust flow.

As shown in Figure 7, the outlet temperature of stenter suction air increases with the increase of exhaust flow rate. As the exhaust temperature increases, the increasing trend of outlet temperature of stenter suction air becomes more sharp. When exhaust flow rate and temperature are 1117 kmol/h and 120 °C, respectively, the outlet temperature of stenter suction air reaches 53 °C, with a temperature difference of 67 °C from the exhaust temperature. When exhaust flow rate is unchanged and the temperature is 210 °C, the outlet temperature of stenter suction air reaches 176 °C, with a temperature difference of 34 °C from the exhaust temperature. This indicates that when recovering waste heat from higher temperature exhaust, increasing the exhaust flow rate has a more prominent effect on raising the stenter suction air outlet temperature. Consequently, the temperature difference between the stenter suction air outlet and the initial exhaust temperature is further reduced. This is advantageous for saving fuel during the subsequent heating of preheated air.

However, a larger exhaust flow rate means a decrease in E1 exergy efficiency, resulting in more exergy losses during the heat exchange process. This indicates that different strategies may be adopted by producers for varying exhaust emission rates. When the produced exhaust is abundant, increasing the exhaust flow rate to pursue a higher stenter suction air outlet temperature can save fuel needed for heating the preheated air. Conversely, when the produced exhaust is insufficient, reducing the exhaust flow rate to decrease the heat transfer temperature difference, retaining more exergy to supply stenter suction air.

For the stenter suction air, the waste heat recovery process should produce more preheated air, but the increase of stenter suction air will lead to the decrease of the outlet temperature of stenter suction air. In order to guide the adjustment of stenter suction air flow rate, the relationship diagram is drawn as shown in Figure 8.

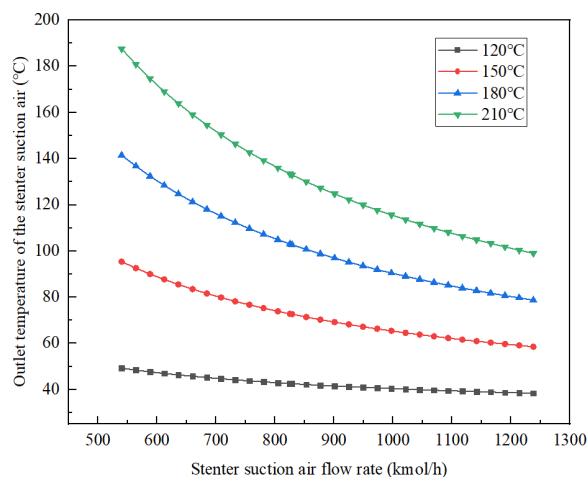


Figure 8. Variation of preheating air outlet temperature with preheating air flow.

As shown in Figure 8, when exhaust temperature is 120 °C, the stenter suction air flow rate increases from 540 kmol/h to 1238 kmol/h, while the outlet temperature decreases from 49 °C to 38 °C correspondingly, a reduction of 11 °C. When exhaust temperature is 210 °C, the outlet temperature decreases from 187 °C to 99 °C for the same range of flow rate, a reduction of 88 °C. This indicates that at higher exhaust temperatures, the trend of decreasing stenter suction air outlet temperature with increasing preheated air flow rate becomes more prominent, whereas at lower exhaust temperatures, this trend is less prominent. The differences in this trend may be related to the energy losses during the heat exchange process at different exhaust temperatures. At higher exhaust temperatures, to maintain a higher stenter suction air outlet temperature, it is advisable to either maintain or decrease the input flow rate of stenter suction air. Conversely, at lower exhaust temperatures, the impact of increasing stenter suction air flow rate on stenter suction air outlet temperature is less significant, allowing for a moderate increase in input flow rate to obtain a larger quantity of stenter suction air.

3.4 Heat Exchanger Design

Aspen EDR is used for the design of heat exchanger, which can provide a better structural design scheme of heat exchanger according to the given process conditions [20].

Common types of heat exchangers used in the textile industry include plate heat exchangers, regenerators, heat pipes, shell-and-tube heat exchangers and so on [21]. In this study, shell-and-tube heat exchangers were chosen. While the thermal efficiency of shell-and-tube heat exchangers may be lower than some other types, taking into consideration factors such as maintenance and lifespan, it remains an acceptable choice. The thermodynamic parameters of each stream which used in heat exchanger design all derived from Results Summary.

Both heat exchangers were designed as BEM type, which is widely used and easy to maintain. The tube side was chosen for the exhaust to improve the heat efficiency. According to the Chinese manufacturing standard, smooth tubes with an outer diameter of 19 mm, a center distance of 25 mm, and a thickness of 2 mm are selected. The fouling thermal resistance of air is obtained as 0.00018 m²·K/W. The remaining settings are set to default.

The TEMA sheet is used to evaluate the heat transfer and hydraulic performance of the heat exchanger. The pressure drop, fluid flow state, ratio of actual heat transfer area to design area, and heat transfer coefficient are four factors that can significantly reflect the heat exchanger performance. High-speed fluid flow contributes to the transfer of heat. However, high fluid velocity can lead to an increase in pressure drop, which not only increases the operating cost of the pump, but also increases irreversible losses in the heat transfer process [22]. A good heat exchanger design needs to balance the effects of flow velocity and heat transfer.

The structural parameters of E1 and E2 are listed in Tables 6, and the operating parameters are listed in Table 7. The structural design diagram of E1 and E2 is shown in Figures 9 and 10.

Table 6. Structural parameters of heat exchanger E1 and E2.

| Name | Units | E1 | E2 |
|-----------------------|-------|------------------|------------------|
| Exchanger type | - | BEM | BEM |
| Material | - | Carbon Steel | Carbon Steel |
| Location of hot fluid | - | Tube side | Tube side |
| Tube OD | mm | 19 | 19 |
| Pitch | mm | 25 | 25 |
| Thickness | mm | 2 | 2 |
| Pattern | - | 30-Triangular | 30-Triangular |
| Number | - | 611 | 1000 |
| Length | mm | 1500 | 3000 |
| Passes | - | 1 | 1 |
| Shell ID | mm | 700 | 1000 |
| OD | mm | 720 | 1020 |
| Passes | - | 1 | 1 |
| Baffle type | - | Single segmental | Single segmental |
| Pitch | mm | 140 | 450 |
| Number | - | 4 | 3 |
| Cut | % | 25 | 40 |

Table 7. Operational parameters of heat exchanger E1 and E2.

| Name | Unit | E1 | | E2 | |
|-------------------------------------|---------------------|-----------|------------|-----------|------------|
| | | Tube side | Shell side | Tube side | Shell side |
| Gross surface area | m ² | 54.7 | | 224.9 | |
| Pressure drop | kPa | 10.27 | 14.53 | 4.94 | 19.46 |
| Inlet Re | - | 37338.90 | 22510.23 | 18680.77 | 31149.20 |
| Outlet Re | - | 38402.45 | 19277.03 | 20947.89 | 27048.94 |
| MTD | °C | 93.87 | | 59.87 | |
| Transfer rate (fouled) | W/m ² ·K | 74.10 | | 57.80 | |
| Actual/Required area ratio (fouled) | - | 3.06 | | 1.79 | |

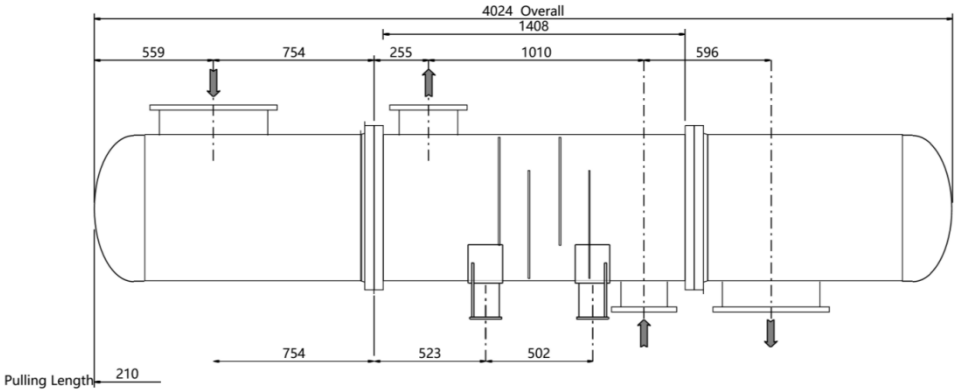


Figure 9. The structure blueprint of heat exchanger E1.

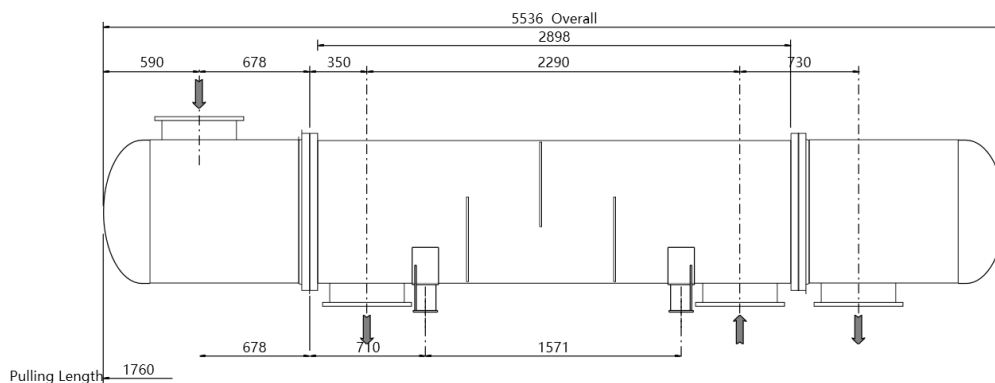


Figure 10. The structure blueprint of heat exchanger E2.

According to the operating parameters of E1 in Table 6, both the pressure drop on tube side and shell side are below 20 kPa. The Reynolds numbers at inlet and outlet of both tube side and shell side are higher than 6000, indicating that the turbulent flow facilitates the heat transfer. The heat exchanger has a compact structure with small inner shell diameters and a tube length of 1500 mm, resulting in a high fluid flow velocity and a high Reynolds number. The heat transfer coefficient of E1 reaches $74.1 \text{ W/m}^2\cdot\text{K}$, indicating a good heat transfer condition. The actual-to-required heat transfer area ratio for the heat exchanger is 3.06, which is much higher than the conventional value of 1.5. Theoretically, a small heat exchange space is enough for the low heat load of 117kW. However, it will cause an unstable flow condition, deteriorating the heat transfer condition and increasing the operating cost of the fans. Considering the small heat transfer area required for this load and the relatively low investment cost of the heat exchanger, a greater area margin is designed.

According to the operating parameters of E2, the heat transfer coefficient is $57.8 \text{ W/m}^2\cdot\text{K}$, which is lower than that of E1. This probably because the Reynolds number at inlet and outlet of tube side fluid is lower, and the flow pattern is smoother, which is related to the larger structure and longer shell radius. The actual-to-required heat transfer area ratio is 1.79, slightly higher than the usual value of 1.5. This is mainly to keep the shell side pressure drop at a lower level by choosing a larger shell radius. This choice may cause a slight decrease in the heat transfer coefficient and an increase in construction cost, but it is beneficial for saving operating cost.

4. Performance of Stenter Exhaust Heat Recovery System

Figure 11 shows the schematic of stenter exhaust treatment technology, which contains waste heat recovery, exhaust adsorption, desorption and catalytic combustion. Compared with Figure 1, the blue and red lines respectively represent the new routes of desorbed air and stenter suction air after adding the waste heat recovery system. Two streams of air from the ambient temperature and the stenter exhaust are successively heat-exchanged in E1 and E2 to obtain a stream of desorbed air at 100°C and a stream of preheated air at 93°C . The preheated air is further heated to 170°C and enters the stenter. The heat generated from the catalytic combustion of concentrated VOCs can be used for other purposes, and the stenter suction air is preheated to save the heating energy consumption. The calculation results show that the heat load and exergy efficiency of E1 are 117 kW and 51% respectively, and those of E2 are 420 kW and 58.9% respectively. This waste heat recovery system improves the overall heat utilization efficiency of stenter exhaust treatment system, reduces the heating energy consumption of the stenter suction air by 44.8%.

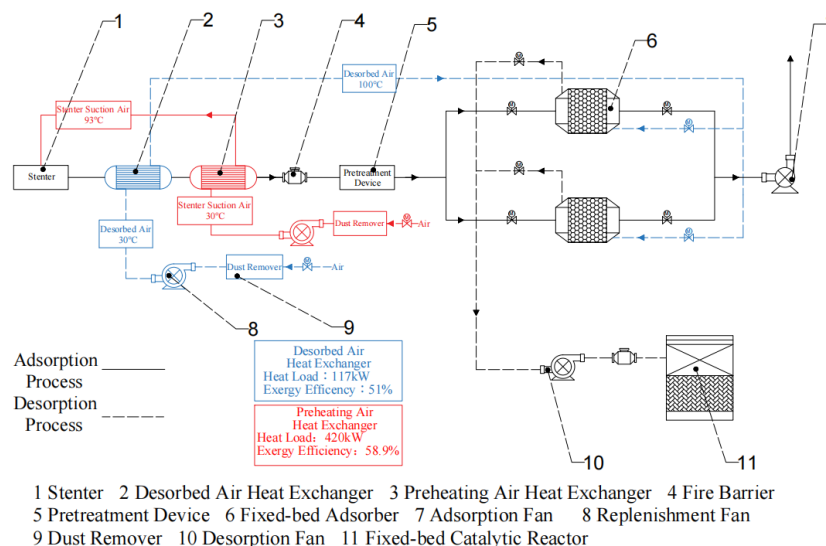


Figure 11. The schematic of the treatment process of stenter exhaust with waste heat recovery system.

Using the method of standard coal heat conversion [23], the annual economic benefit of heat recovery for E1 is calculated to be \$ 19,459, and the annual economic benefit of heat recovery for E2 is \$ 69,853. The total annual economic benefit generated by the heat recovery system is \$ 89,312. Based on the data provided by Aspen Capital Cost Estimator, the material cost of E1 is \$ 7,711, and the material cost of E2 is \$ 63,714, with a total cost of \$ 71,425. With a construction period of 6 months, the static investment payback period is 1.17 years. Therefore, the heat recovery system can generate significant economic benefits each year, with great potential for energy saving.

5. Conclusion

This study focused on the recoverable waste heat of stenter exhaust. Based on the waste gas treatment process, a waste heat recovery scheme for stenter exhaust was proposed, and the waste heat recovery process was established through Aspen Plus simulation. Based on the process data, using exergy analysis to reveal the energy utilization efficiency of waste heat recovery process and further discussing the influence of exhaust flow rate variation on exergy efficiency of heat exchanger under different exhaust temperature. The impacts of exhaust flow rate and stenter suction air flow rate on the heat transfer process were explored. The detailed structure of the heat exchanger was designed. Finally, the economic benefits of waste heat recovery system were evaluated, and the overall energy-saving effect of exhaust waste heat recovery system was demonstrated. The main results obtained could be summarized as follows:

Based on the conditions provided, a stream of 100 °C desorbed air and a stream of 93 °C preheated air can be obtained from the waste heat recovery process. Based on exergy analysis, the exergy efficiency of the desorbed air heat exchanger is 51%, the exergy efficiency of the preheating air heat exchanger is 58.9%.

The Exhaust Exergy Utilization Rate (EUR) for the heat exchange process between desorbed air heat exchanger and preheating air heat exchanger is 8.7% and 30%, respectively. This indicates that the waste heat recovery system can recover close to half of the total exergy from the exhaust.

To increase the exergy efficiency of desorbed air heat exchanger, retain more exergy from the exhaust before the second round of heat exchange, a bypass strategy can be employed. When the exhaust flow rate is 278 kmol/h, the exergy efficiency can achieve 55%, representing a 4% improvement compared to the original exergy efficiency. Considering the differences in desorbed air heat exchanger exergy efficiency at various exhaust temperatures, the 4% increase in exergy efficiency is a substantial benefit.

With the higher exhaust temperature, a large flow rate of the exhaust can increase the outlet temperature of the stenter suction air more significantly, and the effect of stenter suction air flow rate variation on the outlet temperature of stenter suction air is more significant.

When the exhaust temperature is relatively high, increasing the exhaust flow rate can more significantly raise the stenter suction outlet air temperature. Depending on the production flow rate of the exhaust, producers can either increase the exhaust flow rate to pursue a higher stenter suction air outlet temperature or decrease the exhaust flow rate to preserve more exergy for supplying the stenter suction air.

On the other hand, at higher exhaust temperatures, an increase in stenter suction air flow rate will more significantly reduce the stenter suction air outlet temperature. Therefore, it is advisable to either maintain or decrease the flow rate to minimize the reduction in stenter suction air outlet temperature. In contrast, at lower exhaust temperatures, a moderate increase in stenter suction air flow rate can be considered to obtain a larger quantity of stenter suction air.

The utilization of this waste heat recovery system can recover 537 kW of waste heat from stenter exhaust and reduce 44.8% of the heating energy consumption for stenter suction air. Economic evaluation based on standard coal heat conversion shows the total annual economic benefit generated by the heat recovery system is \$ 89,312. The static investment payback period of the waste heat recovery system is 1.17 years.

Author Contributions

Yimin Chen: Investigation, Models creation, Formal analysis, Data curation, Writing - original draft. Bo Liu: Formal analysis, Data Curation, Visualization, Writing - original draft. Zheng Zeng: Conceptualization, Methodology, Project administration, Supervision, Writing - review & editing. Liqing Li: Conceptualization, Methodology, Supervision, Writing - review & editing.

Acknowledgments

This project was supported by the National Key Research and Development Program of China (No. 2019YFC0214302).

Conflict of interest

There is no conflict of interest for this study.

References

- [1] Gao, H.S.; Chen, H.P.; Xu, J.R. Progress in Tenting Machine Waste Gas Treatment Technology. *Text. Dyeing and Finishing J.* **2011**, *33*, 34–38.
- [2] Xu, Z.-R.; Wang, P.; Wang, Z.-M.; Xu, M.-Z.; Wu, J.-B.; Li, Y. Study on the emission characteristics and potential environment hazards of the heat-setting machine of the typical dyeing and finishing enterprise. *Environ. Sci.* **2014**, *35*, 847–52.
- [3] Malakar, S.; Das Saha, P.; Baskaran, D.; Rajamanickam, R. Comparative study of biofiltration process for treatment of VOCs emission from petroleum refinery wastewater—A review. *Environ. Technol. Innov.* **2017**, *8*, 441–461, <https://doi.org/10.1016/j.eti.2017.09.007>.
- [4] Li, Q.; Li, F.-T. Recent advances in surface and interface design of photocatalysts for the degradation of volatile organic compounds. *Adv. Colloid Interface Sci.* **2020**, *284*, 102275, <https://doi.org/10.1016/j.cis.2020.102275>.
- [5] Chang, Z.; Wang, C.; Zhang, G. Progress in degradation of volatile organic compounds based on low-temperature plasma technology. *Plasma Process. Polym.* **2020**, *17*, 1900131, <https://doi.org/10.1002/ppap.201900131>.
- [6] Li, S.X.; Su, J.H.; Ma, D.G. Volatile Organic Compound Pollution Control Engineering. Chemical Industry Press: Beijing, China, 2017, pp. 134–137.
- [7] Sekkeli, M.; Kececioglu, O.F. Scada Based an Energy Saving Approach to Operation of Stenter Machine in a Textile Plant Using Waste Heat Recovery System. *Tekst. Konfeksiyon.* **2012**, *2*, 248–257.
- [8] Zhang, N.; Smith, R.; Bulatov, I.; Klemeš, J.J. Sustaining high energy efficiency in existing processes with advanced process integration technology. *Appl. Energy* **2013**, *101*, 26–32, <https://doi.org/10.1016/j.apenergy.2012.02.037>.
- [9] Patel, N.G.; Shendage, D.J.; Parikh, M.G.; Basu, S.K.; Bade, M.H. Energy model-based benchmarking of the drying process in the stenter machine. *Dry. Technol.* **2021**, *39*, 1114–1133, <https://doi.org/10.1080/07373937.2021.1907401>.

- [10] Rakib, M.I.; Saidur, R.; Mohamad, E.N.; Afifi, A.M. Waste-heat utilization – The sustainable technologies to minimize energy consumption in Bangladesh textile sector. *J. Clean. Prod.* **2017**, *142*, 1867–1876, <https://doi.org/10.1016/j.jclepro.2016.11.098>.
- [11] Gelir, B.C.; Ceylan, H. The effect of the heat recovery on fuel consumption in the stenter machine. *Therm. Sci.* **2021**, *25*, 1047–1055.
- [12] Ozturk, E.; Cinperi, N.C.; Kitis, M. Improving energy efficiency using the most appropriate techniques in an integrated woolen textile facility. *J. Clean. Prod.* **2020**, *254*, 120145, <https://doi.org/10.1016/j.jclepro.2020.120145>.
- [13] Amaris, C.; Miranda, B.; Balbis-Morejón, M. Experimental thermal performance and modelling of a waste heat recovery unit in an energy cogeneration system. *Therm. Sci. Eng. Prog.* **2020**, *20*, 100684, <https://doi.org/10.1016/j.tsep.2020.100684>.
- [14] Chen, T.; Shu, G.; Tian, H.; Zhao, T.; Zhang, H.; Zhang, Z. Performance evaluation of metal-foam baffle exhaust heat exchanger for waste heat recovery. *Appl. Energy* **2020**, *266*, <https://doi.org/10.1016/j.apenergy.2020.114875>.
- [15] Norouzi, A.; Sodagar-Abardeh, J.; Arabkoohsar, A.; Ismail, K.A.R. Investigating thermo-hydraulic behavior of pillow plate heat exchangers using entropy generation approach. *Chem. Eng. Process. - Process. Intensif.* **2022**, *174*, 108887, <https://doi.org/10.1016/j.cep.2022.108887>.
- [16] Han, Y.; Zhang, C.-C.; Zhu, Y.-J.; Wu, X.-H.; Jin, T.-X.; Li, J.-N. Investigation of heat transfer Exergy loss number and its application in optimization for the shell and helically coiled tube heat exchanger. *Appl. Therm. Eng.* **2022**, *211*, 118424, <https://doi.org/10.1016/j.applthermaleng.2022.118424>.
- [17] Etghani, M.M.; Baboli, S.A.H. Numerical investigation and optimization of heat transfer and exergy loss in shell and helical tube heat exchanger. *Appl. Therm. Eng.* **2017**, *121*, 294–301, <https://doi.org/10.1016/j.applthermaleng.2017.04.074>.
- [18] Zhang, L.; Zhai, H.; He, J.; Yang, F.; Wang, S. Application of Exergy Analysis in Flue Gas Condensation Waste Heat Recovery System Evaluation. *Energies* **2022**, *15*, 7525, <https://doi.org/10.3390/en15207525>.
- [19] Guo, J.F.; Zhang, H.Y.; Cui, X.Y.; Huai, X.L.; Han, Z.X.; The Thermal Analysis of Low Grade Flue Gas Heat Recovery Heat Exchanger. *J. Eng. Thermophys.* **2020**, *41*, 39–45.
- [20] Saaedi, M.; Mehrpooya, M.; Shabani, A.; Moosavian, S.M.A. Design and economic analysis of heat exchangers used in solar cogeneration systems based on nanoworking fluid. *Chem. Pap.* **2022**, *76*, 7475–7492, <https://doi.org/10.1007/s11696-022-02427-2>.
- [21] Ogulata, R.T. Utilization of waste-heat recovery in textile drying. *Appl. Energy* **2004**, *79*, 41–49.
- [22] He, L.; Li, P. Numerical investigation on double tube-pass shell-and-tube heat exchangers with different baffle configurations. *Appl. Therm. Eng.* **2018**, *143*, 561–569, <https://doi.org/10.1016/j.applthermaleng.2018.07.098>.
- [23] Sinton, J.E. Accuracy and reliability of China's energy statistics. *China Econ. Rev.* **2001**, *12*, 373–383.